Chemical bonding between host and guest in the $(HgBr_2)_{0.5}Bi_2Sr_{1.5-x}La_xCa_{1.5}Cu_2O_y$ ($x=0.0$, 0.2, and 0.4) superconducting-insulating nanocomposite system

Seong-Ju Hwang, Seung-Joo Kim, and Jin-Ho Choy*
Department of Chemistry, Center for Molecular Catalysis, College of Natural Sciences, Seoul National University, Seoul 151-742, Korea
(Received 12 May 1997)

X-ray-absorption spectroscopic studies have been systematically carried out for the La-substituted $Bi_2Sr_{1.5-x}La_xCa_{1.5}Cu_2O_y$ ($x=0.0$, 0.2, and 0.4) compounds and their $HgBr_2$ intercalates in order to characterize the variation of the chemical bonding nature of host and guest upon substitution and intercalation reactions. According to the Cu K-edge x-ray-absorption near-edge structure-extended x-ray-absorption fine-structure analyses, it is found that the oxidation state of the CuO_2 layers is reduced by substituting the Sr^{+II} ion with La^{+III}, while it is enhanced by the intercalation of $HgBr_2$. Such findings provide clear evidence of the main role of charge transfer in determining the T_c of the intercalate. The chemical bonding between host lattice and intercalant layer has also been investigated by performing the Br K-edge and Hg L_{III}-edge x-ray-absorption spectroscopic analyses, indicating that a small fraction of electrons are transferred from host to guest and that the bond strength of Hg-Br as well as of Br-Bi is changed as the La-substitution rate increases. These results underline that the local substitution of La^{+III} ions into the SrO plane gives rise to the overall changes for all the chemical bonds in these superconducting lattices and clarify that the competing bond model can be effectively applied to the chemically substituted superconducting oxides. [S0163-1829(98)02805-7]

I. INTRODUCTION

Recently, we have developed mercuric-halide-intercalated $Bi_2Sr_2CaCu_2O_y$ compounds $(HgX_2)_{0.5}Bi_2Sr_2CaCu_2O_y$ ($X=$Br and I), which are very interesting due to their unique hybridized crystal structure.[1] In such nanocomposites, superconducting $Bi_2Sr_2CaCu_2O_y$ blocks are alternatively interstratified with electronically insulating HgX_2 layers. In this respect, the intercalation of the HgX_2 molecule into a $Bi_2Sr_2CaCu_2O_y$ lattice is expected to minimize the electronic coupling between adjacent superconducting blocks and consequently to enhance the two dimensionality not only in its crystal structure itself, but also in its electron conduction process.[2] In fact, our previous magnetization study showed clearly that the positional fluctuation of a vortex is significantly increased upon HgX_2 intercalation even at far below the transition temperature (T_c), indicating a remarkable weakening of the interblock interaction.[3] For this reason, the mercuric halide intercalates have been revealed to be good model compounds for examining the contribution of interblock coupling to the high-T_c superconductivity of layered copper oxides.

More recently, we have performed the intercalation of $HgBr_2$ into $Bi_2Sr_{1.5-x}La_xCa_{1.5}Cu_2O_y$ ($0.0\leqslant x\leqslant 0.4$) superconductors[4] in which the hole concentration in the CuO_2 layer is controlled by substituting an alliovalent La^{+III} cation for a Sr^{+II} one[5–10] in order to compare the T_c changes between hole-underdoped samples and hole-overdoped ones upon $HgBr_2$ intercalation. If the T_c variation upon intercalation is due to a weakening of interblock coupling owing to the basal increment, T_c is expected to decrease equally regardless of the hole concentration, while if the T_c change is due to the hole doping by charge transfer, the maximum T_c will shift to the hole-underdoped region for attaining the optimum hole concentration. From magnetic susceptibility measurements, it was found that the $HgBr_2$ intercalation depresses the T_c's of overdoped pristines by $<\sim 6$ K, but increases those of underdoped ones by 4–6 K, indicating the hole doping from intercalant layer to host lattice. Therefore, it was concluded that the change of electronic structure in a CuO_2 layer is primarily responsible for the T_c variation after intercalation rather than the interblock coupling effect.

In the present study, we have carried out systematically x-ray-absorption spectroscopic (XAS) analyses for La-substituted $Bi_2Sr_{1.5-x}La_xCa_{1.5}Cu_2O_y$ compounds with $x=0.0$, 0.2, and 0.4 and their $HgBr_2$ intercalates, in order not only to confirm the earlier conclusion about the origin of the T_c variation upon intercalation, but also to probe the evolution of the chemical bonding nature induced by substitution and intercalation reactions, and to investigate their relationship with superconducting properties. Even though it is certain that T_c of cuprate superconductors is closely related to the hole concentration of CuO_2 layers,[6] there might be other parameters affecting the superconducting properties such as the Cu-O bond distance. As clearly observed in the La-Sr-Cu-O system, it has been well known that the high-T_c superconducting copper oxides including Bi-based cuprates behave like Mott-Hubbard insulators in the region of low carrier concentration and like superconductors in the intermediate ranges, while in the heavily doped region they are normal-metal-like.[11–13] And this characteristic phase transition has been interpreted within the context of a relation between U and W, where U is the intra-atomic correlation energy and W is the width of valence band, which is strongly dependent on the crystal structure of CuO_2 layers.[14] In this respect, the Cu K-edge extended x-ray-absorption fine-structure (EXAFS) analyses for La-substituted pristines and their intercalates might provide useful information about the relationship between the width of the valence band and the superconductivity in layered copper oxides, along with the

variation of hole concentration. And our interests are extended to chemical environments of La^{+III}, since the incorporation of a La^{+III} ion into the SrO plane is expected to induce a significant change in the adjacent chemical bonds. Such a change has appeared to be a challenge in applying the competing bond model to high-T_c superconducting materials.[15–17] A precise understanding of the effect of chemical substitution is thought to be very useful in studying and designing high-T_c materials, since high-T_c superconductivity in metal oxides has often been achieved through the substitution of an alliovalent cation as in the La-Ba-Cu-O and Nd-Ce-Cu-O systems.[18,19]

II. EXPERIMENT

Polycrystalline samples of $Bi_2Sr_{1.5-x}La_xCa_{1.5}Cu_2O_y$ with $0.0 \leqslant x \leqslant 0.4$ have been synthesized by the conventional solid-state reaction method and their $HgBr_2$ intercalates by heating pristine polycrystals with mercuric bromide in vacuum-sealed Pyrex tubes as described previously, and then characterized by powder x-ray-diffraction (XRD) analysis and thermogravimetric analysis (TGA).[4] We have chosen compounds only with the substitution rate of $x = 0.0$, 0.2, and 0.4 for performing the XAS experiments, since they represent the hole-overdoped, optimally doped, and -underdoped states, respectively.

The present XAS spectra were measured with synchrotron radiation by using EXAFS facilities, installed at the beam line 10B at the Photon Factory, National Laboratory for High Energy Physics in Tsukuba, operated at 2.5 GeV and 260–370 mA.[20] The samples were finely ground, mixed with boron nitride (BN) in an appropriate ratio, and pressed into pellets in order to obtain an optimum absorption jump ($\Delta\mu t \approx 1$), enough to be free from thickness and pin-hole effects.[21,22] All the present spectra were obtained at room temperature in a transmission mode using gas-ionization detectors with a spacing of ~ 0.4 eV for the x-ray-absorption near-edge structure (XANES) region and ~ 1.5 eV for the EXAFS one. The silicon (311) channel-cut monochromator was used for the Cu K, Hg L_{III}, Bi L_{III}, and Br K edges. To ensure the reliability of the spectra, much care has been taken to evaluate the stability of the energy scale by monitoring the spectra of Cu metal and Bi_2O_3 for each measurement and thus edge positions were reproducible to better than 0.05 eV.

The data analysis for the present spectra was performed by the standard procedure as reported previously.[1] All the present XANES spectra were normalized by fitting the smooth EXAFS high-energy region with a linear function after subtracting the background extrapolated from the pre-edge region. In the case of the Br K edge (13 470 eV), a perturbation from the adjacent Bi L_{III} edge (13 426 eV) was removed by subtracting the Bi L_{III}-edge spectrum of HgI_2 intercalate from the perturbed original spectra.[1] The EXAFS oscillations were separated from the absorption background by using a cubic spline background removal technique. The resulting $\chi(k)$ oscillations were weighted with k^3 in order to compensate for the diminishing amplitude of the EXAFS at the high-k region. For analyzing the EXAFS data, a nonlinear least-squares curve fitting was carried out to the Fourier-filtered first coordination shell by minimizing the value of F ($F = [\Sigma k^6(\chi_{\mathrm{cal}} - \chi_{\mathrm{expt}})^2]^{1/2}/n$, where the summation was performed over the data points (n) in the analyzed k range) with the use of well-known single-scattering EXAFS theory.[23]

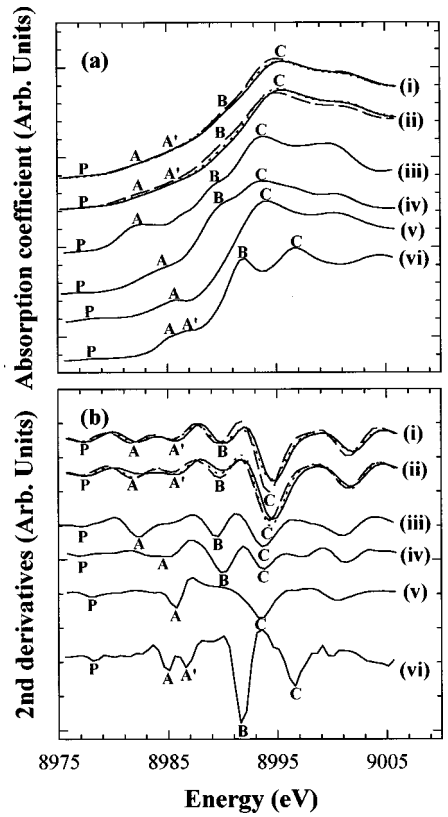

FIG. 1. Cu K-edge XANES (a) spline and (b) second-derivative spectra for (i) the pristines $Bi_2Sr_{1.5-x}La_xCa_{1.5}Cu_2O_y$ with $x = 0.0$, 0.2, and 0.4, (ii) their $HgBr_2$ intercalates, (iii) Nd_2CuO_4, (iv) La_2CuO_4, (v) $LaCuO_3$, and (vi) $La_2Li_{0.5}Cu_{0.5}O_4$. For (i) and (ii), the solid, dotted, and dashed lines represent the pristines and intercalates with $x = 0.0$, 0.2, and 0.4, respectively. In case of the Bi-based cuprates, the second derivatives were multiplied by 2 in order to represent clearly the spectral changes upon La substitution.

III. RESULTS AND DISCUSSION

Figure 1 represents the Cu K-edge XANES spline and second-derivative spectra for the pristines $Bi_2Sr_{1.5-x}La_xCa_{1.5}Cu_2O_y$ ($x = 0.0$, 0.2, and 0.4) and their $HgBr_2$ intercalates, together with those for reference of Nd_2CuO_4, La_2CuO_4, $LaCuO_3$, and $La_2Li_{0.5}Cu_{0.5}O_4$, where divalent or trivalent copper ion is stabilized in the different local geometries. It is found that the edge energies of Bi-based cuprates are lower than those of Cu^{+III} references, but higher than those of Cu^{+II} ones, indicating the mixed oxidation state of copper (Cu^{+II}/Cu^{+III}) in these compounds. In comparing the spectra of the pristines, there is an overall shift toward lower energy as the Sr^{+II} ion is substituted by a La^{+III} one, indicating that the hole concentration of the CuO_2 layer is effectively reduced. And this is consistent with the parabolic feature of the plot of T_c vs x as previously reported.[4] In order to get detailed information on the electronic and geometric structures of the copper-oxygen layer, each spectrum has been carefully investigated by using the second-differential method which is quite effective in differ-

entiating a small difference of spectral features [Fig. 1(b)].[21] A small pre-edge peak (denoted as P) is observed commonly for all the present compounds, which is assigned to the quadrupole-allowed transition from the core $1s$ level to the unoccupied $3d$ state.[24] The energy of this peak for the Bi-based cuprates is found to be slightly lower than that for the Cu^{+III} references, but higher than that for the Cu^{+II} ones, confirming again the presence of mixed-valent copper in the lattice. In the main-edge region, there are some peaks corresponding to the dipole-allowed transitions from the core $1s$ level to unoccupied $4p$ states, which are denoted as A, B, and C. According to our previous Cu K-edge XAS study,[25] the main-edge features A and B are attributed to the transitions from the $1s$ orbital to the out-of-plane $4p_\pi$ one with and without shakedown processes,[26] respectively, whereas the feature C is ascribed to an in-plane $4p_\sigma$ orbital transition without a shakedown process. In the case of $La_2Li_{0.5}Cu_{0.5}O_4$ where the trivalent copper ion is stabilized in the anisotropic crystal field, the shakedown peak A is separated into A and A' peaks, those which correspond to $1s^23d^8 \rightarrow 1s^13d^94p_\pi{}^1L$ and $1s^23d^8 \rightarrow 1s^13d^94p_\sigma{}^1L$ transitions, respectively. Since the shakedown process to the $4p_\sigma$ orbital occurs exclusively for the trivalent copper compound, the peak A' has been revealed as an indicator for the presence of Cu^{+III} species. In fact, this peak has been effectively applied for investigating the oxidation state of copper in chemically and electrochemically prepared $La_2CuO_{4.08}$.[27] It is clearly observed from Fig. 1(b) that peak A' is significantly depressed with an increase of the La substitution rate (x), whereas peak A relating to the Cu^{+II} ion is enhanced, which is in good agreement with the shift of the edge energy. However, there is no remarkable change in the Cu K-edge XANES spectra before and after intercalation of $HgBr_2$, suggesting that the modification of electronic structure in the CuO_2 layer is too weak to be observed. Actually, the Cu K-edge XANES spectrum cannot reflect sensitively such a small change since it does not probe the orbital with d character that is directly involved in the chemical bonding. However, it is expected that such a slight modification of the electronic structure could be detected by measuring the (Cu-O) bond distances. In this respect, the Cu K-edge EXAFS analyses have also been carried out for the pristines and their intercalates in order to determine the evolution of local structure around copper upon intercalation.

The k^3-weighted EXAFS spectra for pristine $Bi_2Sr_{1.5-x}La_xCa_{1.5}Cu_2O_y$ ($x=0.0$, 0.2, and 0.4) and their $HgBr_2$ intercalates were Fourier transformed in the k range of 2.6–12.8 $Å^{-1}$ as shown in Fig. 2(a).[28] The first prominent peak in the Fourier transform (FT) corresponding to the in-plane and out-of-plane (Cu-O) pairs was isolated by inverse Fourier transform to k space.[29–31] The resulting $k^3\chi(k)$ Fourier-filtered EXAFS oscillations are represented in Fig. 2(b), and the curve fittings were carried out to them in order to determine the structural parameters such as coordination number (N), bond length [R(Hg-X)], and Debye-Waller factor (σ^2). The best fitting results to the first coordination shell are compared to the experimental spectra in Fig. 2(b), and the fitted structural parameters are listed in Table I. The in-plane and out-of-plane (Cu-O) bond distances for the pristines and their $HgBr_2$ intercalates are plotted as a function of

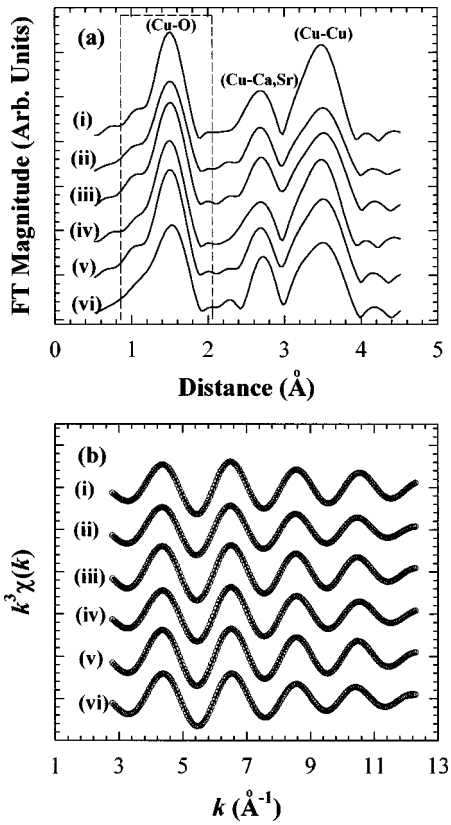

FIG. 2. (a) Fourier-transformed Cu K-edge EXAFS spectra and (b) their inverse Fourier transforms of (i) $Bi_2Sr_{1.5}Ca_{1.5}Cu_2O_y$, (ii) $Bi_2Sr_{1.3}La_{0.2}Ca_{1.5}Cu_2O_y$, (iii) $Bi_2Sr_{1.1}La_{0.4}Ca_{1.5}Cu_2O_y$, (iv) $(HgBr_2)_{0.5}Bi_2Sr_{1.5}Ca_{1.5}Cu_2O_y$, (v) $(HgBr_2)_{0.5}Bi_2Sr_{1.3}La_{0.2}Ca_{1.5}Cu_2O_y$, and (vi) $(HgBr_2)_{0.5}Bi_2Sr_{1.1}La_{0.4}Ca_{1.5}Cu_2O_y$. In (a), the range over which the Fourier filtering has been made is shown by the dashed lines. In (b), the solid lines and open circles represent the fitted and experimental data, respectively.

the La substitution rate (x) in Fig. 3. There is an increasing trend of the in-plane Cu-O_p bond distance for the pristines and their intercalates with an increase of La content, indicating the reduction of the CuO_2 layer due to electron doping by La substitution. This is consistent with an increase of the a-axis lattice parameter determined from powder XRD analysis and the shift of the edge energy in the Cu K-edge XANES spectra. In contrast to a small variation in the in-plane bond distance, we can observe a significant decrease in the out-of-plane Cu-O_{Sr} bond distance by substituting a La^{+III} ion for a Sr^{+II} one, which is also in good agreement with a decrease of the c-axis lattice parameter. In principle, there are two competitive factors affecting the Cu-O_{Sr} bond distance. One is the size factor where the crystal lattice is contracted by replacing a larger Sr^{+II} ion with a smaller La^{+III} one[32] [$Sr^{+II}(8)=1.25$ Å, $La^{+III}(8)=1.18$ Å, where the number in parentheses represents the coordination number], and the other is the electronic factor where the substitution of a higher-valent La^{+III} cation results in a decrease of the average oxidation state of the CuO_2 sheet; consequently, the Cu-O_{Sr} bond is elongated due to a decrease of covalency. The observed bond contraction upon La substitution indicates clearly that the former factor plays a more important role in determining the Cu-O bond distance rather than the

TABLE I. Results of a nonlinear least-squares curve fitting for the first shell of Cu K-edge EXAFS spectra for the pristines $Bi_2Sr_{1.5-x}La_xCa_{1.5}Cu_2O_y$ and their $HgBr_2$ intercalates.

		$x=0$		$x=0.2$		$x=0.4$	
Parameter		Pristine	Intercalate	Pristine	Intercalate	Pristine	Intercalate
R (Å)	Cu-O_{eq}	1.90_1	1.90_0	1.91_3	1.91_0	1.91_4	1.91_4
	Cu-O_{ax}	2.36_4	2.34_8	2.34_3	2.32_5	2.32_1	2.29_8
σ^2	Cu-O_{eq}	3.2_0	4.0_6	4.5_3	4.1_1	4.3_6	6.3_3
(10^{-3} Å^2)	Cu-O_{ax}	4.7_0	4.4_1	8.8_4	11.2_5	10.8_8	7.1_1
CN[a]	Cu-O_{eq}	4	4	4	4	4	4
	Cu-O_{ax}	1	1	1	1	1	1

[a]The coordination number was fixed to the crystallographic value due to a strong correlation between the Debye-Waller factor and coordination number.

latter. In the case of $HgBr_2$ intercalate, the out-of-plane bond distance is found to decrease remarkably compared to that of the pristine, whereas the in-plane one is not significantly changed. Since the La content remains constant during the intercalation reaction, the aforementioned size factor can be excluded as an origin of the change in bond length. Therefore, the shrinkage of the Cu-O_{Sr} bond induced by intercalation is surely due to an electronic factor, implying that the copper ion is oxidized by charge transfer between the host CuO_2 layer and guest $HgBr_2$ along the Cu-O_{Sr} and Bi-O_{Sr} bonds.[33] Moreover, the difference in the Cu-O_{Sr} bond distance between pristines and intercalates is determined to be nearly constant in all substitution ranges, indicating that the structural evolution of the CuO_2 layer is independent of La substitution.

From the viewpoint of electronic structure, the variation of the Cu-O bond distance gives rise to a change in the width of the valence band (W). In a tight-binding approximation,[34] W is given as $W \approx 8b \sim \varepsilon_\sigma(\lambda_\sigma^2+\lambda_s^2)$, where b is the spin-independent electron transfer energy integral (resonance integral) for nearest-neighbor copper atoms, ε_σ is the one-electron energy, and λ_σ (or λ_s) is the covalent-mixing parameter, λ_σ (or λ_s) $\equiv b^{ca}/\Delta E$ for electron transfer from an O $2p_\sigma$ (or O $2s$) orbital to an empty Cu $3d_{x^2-y^2}$ one with a cation-anion resonance integral b^{ca} and energy difference between two orbitals ΔE. When the apical Cu-O bond becomes shorter, it is expected that the Coulombic repulsion between c-axis oxide ions and basal-plane ones will be remarkably enhanced, and thereby the Madelung stabilization of O $2p$ orbitals becomes weaker.[35] Since the O $2p$ orbital lies below the empty Cu $3d_{x^2-y^2}$ one,[36] ΔE is lowered and W becomes larger. For $YBa_2Cu_4O_8$, an increase in T_c with hydrostatic pressure has been found to be correlated with a decrease in the c-axis parameter and Cu(2)-O bond.[37] In contrast, the T_c of the hole-overdoped compound $Tl_{2-y}Ba_2CuO_{6-x}$ has been revealed to be depressed with a decrease of the c-axis parameter and with an increase of the bandwidth.[38] Together with the above examples, the present Cu K-edge EXAFS results indicate clearly that the contraction of the copper-axial oxygen bond gives rise to a different T_c variation depending upon the hole concentration of the CuO_2 layer; that is, it enhances the T_c of the underdoped compound ($x=0.4$), but depresses that of the overdoped one ($x=0.0$). On the basis of such findings, it is suggested that the T_c of the superconducting material can be optimized by controlling the axial Cu-O bond distance through chemical substitution.

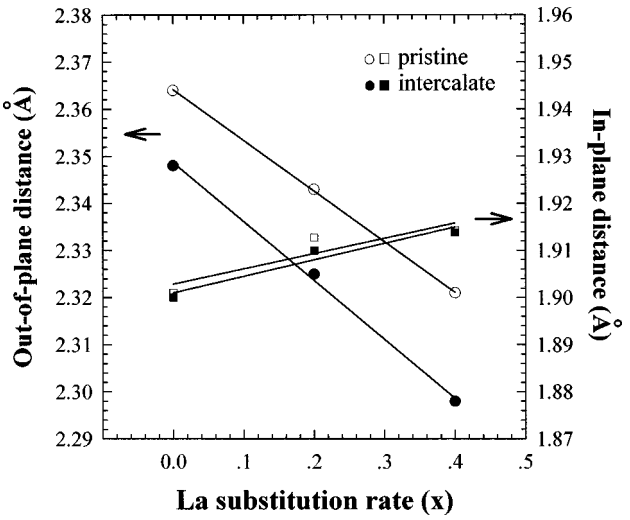

FIG. 3. Variation of in-plane Cu-O bond distances (cubes) and out-of-plane ones (circles) as a function of La content for the pristines (open symbols) and their $HgBr_2$ intercalates (solid symbols).

Figures 4(a) and 4(b) represent the Bi L_{III}-edge XANES spline and second-derivative spectra for the pristines and their $HgBr_2$ intercalates, respectively, together with those for the reference Bi_2O_3. There are three broad peaks, indicated as A, B, and C, in all the present spectra and their energies are summarized in Table II. Among them, the pre-edge peak A is assigned to the $2p_{3/2} \rightarrow 6s$ transition, while the higher main-edge peaks B and C are attributed to $2p_{3/2} \rightarrow 6d_{t_{2g}}$ and $2p_{3/2} \rightarrow 6d_{e_g}$ ones, respectively.[39–41] It is clearly seen that the energy difference between peaks B and C is diminished upon intercalation as listed in Table II. Since this peak splitting is surely proportional to the strength of the crystal field,[1] the observed decrease in energy difference (ΔE_{t2g-e_g}) reflects the weakening of the crystal field around bismuth upon intercalation, which is thought to originate from the following two effects. One is the effect of introducing guest molecules in between the Bi_2O_2 double layer where axially coordinated oxygen in an adjacent BiO layer (O_{Bi}) is replaced by bromine. Since the electronegativity of bromine is smaller than that of oxygen, the strength of the crystal field around

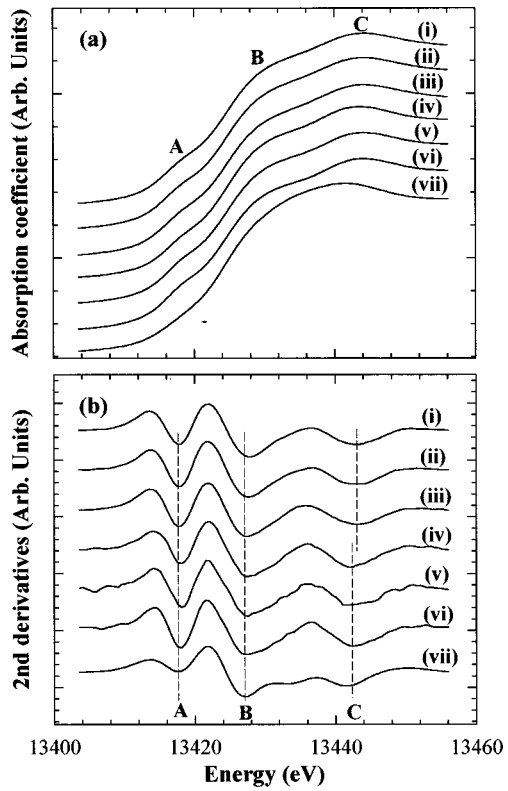

FIG. 4. Bi L_{III}-edge XANES (a) spline and (b) second-derivative spectra for (i) $Bi_2Sr_{1.5}Ca_{1.5}Cu_2O_y$, (ii) $Bi_2Sr_{1.3}La_{0.2}Ca_{1.5}Cu_2O_y$, (iii) $Bi_2Sr_{1.1}La_{0.4}Ca_{1.5}Cu_2O_y$, (iv) $(HgBr_2)_{0.5}Bi_2Sr_{1.5}Ca_{1.5}Cu_2O_y$, (v) $(HgBr_2)_{0.5}Bi_2Sr_{1.3}La_{0.2}Ca_{1.5}Cu_2O_y$, (vi) $(HgBr_2)_{0.5}Bi_2Sr_{1.1}La_{0.4}Ca_{1.5}Cu_2O_y$, and (vii) Bi_2O_3.

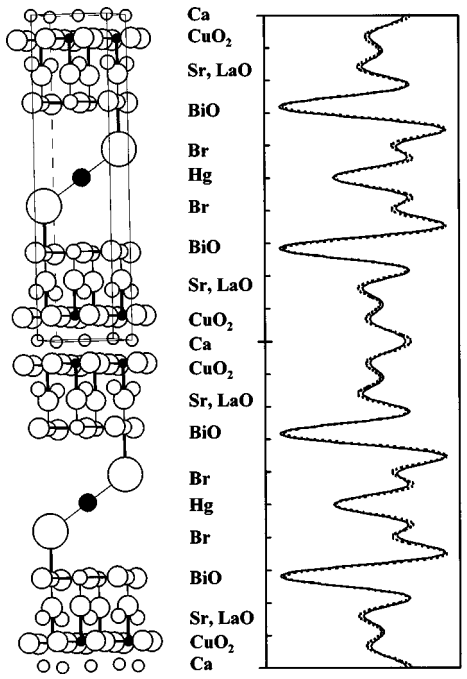

FIG. 5. Schematic representation for the evolution of chemical bonds in the $(HgBr_2)_{0.5}Bi_2Sr_{1.5-x}La_xCa_{1.5}Cu_2O_y$ compound upon La substitution, together with one-dimensional electron density maps along the *c* axis. In structural model, the boldface and lightface solid lines represent the reinforced and weakened bonds upon La substitution, respectively. In the electron density map, the dotted and solid lines represent the calculated electron density based on the observed XRD patterns and that on the basis of the present crystal structure, respectively.

the bismuth ion decreases. And the other is the effect of increasing the Bi-O_{Sr} bond distance which can be well expected from the Cu *K*-edge EXAFS results. As shown in Fig. 5, because the axial oxygen is coordinated to a copper ion in one direction and to a bismuth ion in the other one, a remarkable shortening of the Cu-O_{Sr} bond results in an increase of the competing Bi-O_{Sr} bond distance and thus a weakening of the crystal field around Bi. But it should be noted that there is another crystal position for the bismuth cation which is not capped by bromine. However, in the case of such an uncapped Bi site, the $HgBr_2$ intercalation is also expected to give rise not only to the weakening of the crystal field around Bi, but to the decrease of the Cu-O_{Sr} bond as in a capped Bi site, on the basis of the following reasons. At first, the out-of-plane bond between Bi and oxygen in an adjacent BiO layer is remarkably elongated by intercalating $HgBr_2$ molecules into interlayer space, which results in a weakening of the crystal field around Bi. On the other hand, since a hole transferred from the intercalated $HgBr_2$ layer would be delocalized over the entire CuO_2 plane, to some extent, the Cu-O_{Sr} bond is also expected to be shortened, even bonded with an uncapped Bi site, which induces the elongation of the competing bond between O_{Sr} and *trans*-positioned uncapped Bi. In fact, there might be some differences in the environment of CuO_2 and BiO layers depending on whether Bi is capped or not. But as described above, the chemical bonds of Cu-O_{Sr} and Bi-O_{Sr} are considered to exhibit a similar response to the $HgBr_2$ intercalation regardless of Br coordination to Bi. Therefore, the present XANES-EXAFS re-

TABLE II. Peak energies of the Bi L_{III}-edge XANES spectral feature for the pristines $Bi_2Sr_{1.5-x}La_xCa_{1.5}Cu_2O_y$ and their $HgBr_2$ intercalates.

Compound	A (eV)[a]	B (eV)[a]	C (eV)[a]	C-B (eV)[a]
$Bi_2Sr_{1.5}Ca_{1.5}Cu_2O_y$	13417.7	13428.0	13442.9	14.9
$(HgBr_2)_{0.5}Bi_2Sr_{1.5}Ca_{1.5}Cu_2O_y$	13418.0	13428.0	13442.4	14.4
$Bi_2Sr_{1.3}La_{0.2}Ca_{1.5}Cu_2O_y$	13417.7	13427.6	13443.3	15.7
$(HgBr_2)_{0.5}Bi_2Sr_{1.3}La_{0.2}Ca_{1.5}Cu_2O_y$	13418.2	13427.6	13442.5	14.9
$Bi_2Sr_{1.1}La_{0.4}Ca_{1.5}Cu_2O_y$	13417.7	13427.4	13443.2	15.8
$(HgBr_2)_{0.5}Bi_2Sr_{1.1}La_{0.4}Ca_{1.5}Cu_2O_y$	13417.8	13427.4	13442.6	15.2

[a]Peak energies were determined from the peak position of the second derivatives.

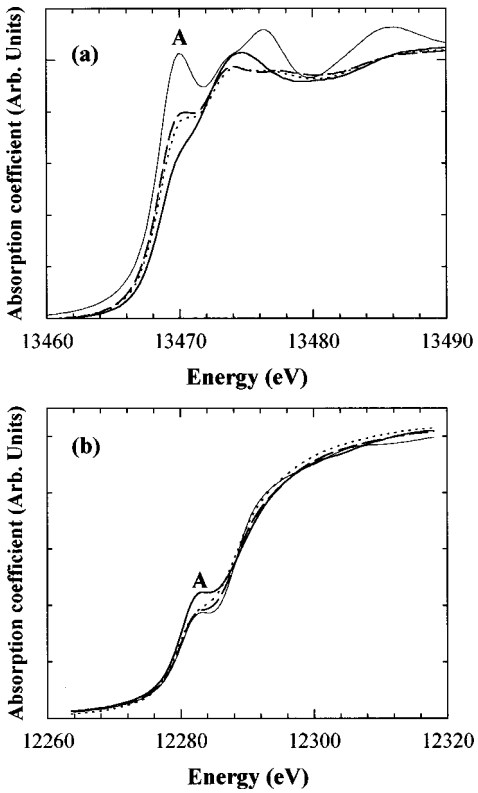

FIG. 6. (a) Br K-edge and (b) Hg L_{III}-edge XANES spectra for $(HgBr_2)_{0.5}Bi_2Sr_{1.5}Ca_{1.5}Cu_2O_y$ (boldface solid lines), $(HgBr_2)_{0.5}Bi_2Sr_{1.3}La_{0.2}Ca_{1.5}Cu_2O_y$ (boldface dotted lines), $(HgBr_2)_{0.5}Bi_2Sr_{1.1}La_{0.4}Ca_{1.5}Cu_2O_y$ (boldface dashed lines), and $HgBr_2$ (lightface solid lines).

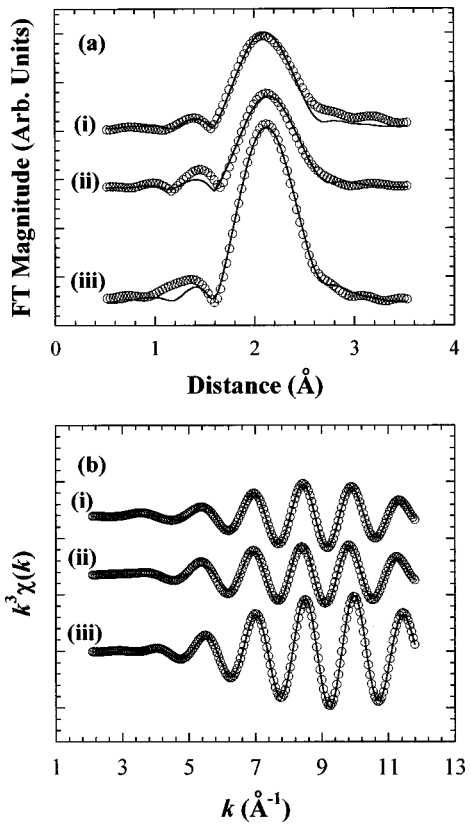

FIG. 7. (a) Fourier-transformed Hg L_{III}-edge EXAFS spectra and (b) their inverse Fourier transforms of (i) $(HgBr_2)_{0.5}Bi_2Sr_{1.5}Ca_{1.5}Cu_2O_y$, (ii) $(HgBr_2)_{0.5}Bi_2Sr_{1.1}La_{0.4}Ca_{1.5}Cu_2O_y$, and (iii) $HgBr_2$. The solid lines and open circles represent the fitted and experimental data, respectively.

sults correspond to averaged variations of the Cu-O_{Sr} bond distance and of the crystal field around Bi.

The Br K-edge XANES spectra for $HgBr_2$ intercalates and free $HgBr_2$ are represented in Fig. 6(a). All the present spectra exhibit a pre-edge peak A (so-called ''white-line''-type feature) around 13 470 eV, assigned to the transition from the $1s$ core level to the $4p$ state above the Fermi energy level (E_F). Although $HgBr_2$ has a formal oxidation state of Br^-, there is a distinct pre-edge peak attributed to the formation of a partially empty $4p$ state resulting from a mixing between Hg $6s$ and Br $4p_z$ orbitals, which is expected from a higher polarizability of Hg^{+II} ion with an electronic configuration of $[Xe]4f^{14}5d^{10}6s^0$, where d and f electrons shield the nucleus poorly.

The intensity of the pre-edge peak A is observed to decrease upon $HgBr_2$ intercalation, indicating that the intercalant $HgBr_2$ layer receives electrons from the host lattice. And it is also found that the extent of peak depression becomes less prominent with an increase of La content, suggestive of the different amount of charge transfer depending on the La substitution rate. However, the present Cu K-edge EXAFS results show obviously that the effect of intercalation on the electronic structure of CuO_2 layers is nearly the same for all substitution ranges. Therefore, the intensity variation of peak A upon La substitution should be explained on the basis of competing bond models. As illustrated in Fig. 5, the La substitution gives rise to a shortening of the Cu-O_{Sr} bond distance, and thereby the competing Bi-O_{Sr} bond is elongated. In turn, a weakening of the Bi-O_{Sr} bond leads to a reinforcement of the competing Bi-Br bond, which allows us to explain the observed decrease in peak intensity with an increase of the substitution rate.

The effect of La substitution on the intracrystalline structure of $HgBr_2$ layers was also examined by performing Hg L_{III}-edge XANES-EXAFS analyses. Figure 6(b) represents the Hg L_{III}-edge XANES spectra of $HgBr_2$ intercalates and unintercalated $HgBr_2$ reference. Since the Hg^{+II} ion has vacant $6s$ and $6d$ orbitals, it is therefore expected that two spectral features should appear corresponding to a $2p_{3/2}\rightarrow 6d$ transition (main-edge peak) and to the $2p_{3/2}\rightarrow 6s$ one (pre-edge peak A), respectively, for all the $HgBr_2$ intercalates including the reference $HgBr_2$.[42,43] As reported,[42] a distinct pre-edge peak appears exclusively for the Hg compounds with linear symmetry, but not for those with different geometries like trigonal planar, tetrahedral, and distorted octahedral ones. In this respect, an enhancement of pre-edge peak A upon intercalation suggests strongly a change in local structure around mercury from an octahedral symmetry to a linear one.

The Fourier transformed Hg L_{III}-edge EXAFS spectra for the $HgBr_2$ intercalates and free $HgBr_2$ are shown in Fig. 7(a).[28] The first peak in the FT is attributed to the mercury-bromine bonding pair, which is isolated by inverse Fourier transformation into k space. The resulting $k^3\chi(k)$ Fourier-filtered EXAFS oscillations are represented in Fig. 7(b), together with the best fits, and the fitted structural parameters

TABLE III. Results of a nonlinear least-squares curve fitting for the first shell of Hg L_{III}-edge EXAFS spectra.

Compound	Parameter	Bond distance (Å)	Coordination number	Debye-Waller factor (10^{-3} Å^2)
$HgBr_2$		2.45_9	$2+4$[a]	3.09
$(HgBr_2)_{0.5}Bi_2Sr_{1.5}Ca_{1.5}Cu_2O_y$		2.46_2	1.85_7	6.41
$(HgBr_2)_{0.5}Bi_2Sr_{1.1}La_{0.4}Ca_{1.5}Cu_2O_y$	2.48_8	1.84_6	6.35	

[a]The coordination number of the reference $HgBr_2$ was fixed to the crystallographic value in order to determine the amplitude reduction factor. The fitting analysis was carried out for the first shell of the $HgBr_6$ octahedron.

are summarized in Table III. The coordination number is determined to be 2 for the intercalates with $x=0.0$ and 0.4, indicating that the mercuric bromide intercalated into a host lattice is stabilized in the form of a linear molecule as in the gaseous state, regardless of La^{+III} content.[44] And it is also found that the Hg-Br bond distance increases from 2.46_2 Å of $(HgBr_2)_{0.5}Bi_2Sr_{1.5}Ca_{1.5}Cu_2O_y$ to 2.48_8 Å of $(HgBr_2)_{0.5}Bi_2Sr_{1.1}La_{0.4}Ca_{1.5}Cu_2O_y$, pointing to the weakening of the Hg-Br bond upon La substitution. This is also in good agreement with an expectation based on the competing bond model where the La substitution enhances the bond strength of Bi-Br, therefore, the competing Hg-Br bond is elongated as shown in Fig. 5. Such a result underlines that the local substitution of a La^{3+} ion into the SrO plane induces overall changes for all the chemical bonds. In this respect, it is very important to consider the effect of local substitution over all the present chemical bonds in studying the physical properties of cation-substituted superconducting materials.

IV. CONCLUSION

In the present study, an attempt has been made to investigate the effect of substitution and intercalation reactions on the electronic and crystal structures of host and guest by performing the systematic XANES and EXAFS analyses for the $Bi_2Sr_{1.5-x}La_xCa_{1.5}Cu_2O_y$ ($x=0.0$, 0.2, and 0.4) compounds and their $HgBr_2$ intercalates. According to the Cu K-edge EXAFS analyses, the Cu-O_{Sr} bond is found to be remarkably shortened upon intercalation for all the La-substituted phases, reflecting the oxidation of the CuO_2 layer. It is therefore concluded that the evolution of T_c upon intercalation is surely related to the variation of hole concentration rather than the weakening of interblock coupling. From the viewpoint of electronic structure, the shortening of the Cu-O_{Sr} bond implies the broadening of the valence band, which is revealed to induce different T_c changes depending upon the hole concentration of the CuO_2 layer, that is, T_c enhancement for the underdoped compound, whereas T_c depression for the overdoped one. Therefore, it is suggested that the T_c of the superconducting material can be optimized by controlling the axial Cu-O bond distance through chemical substitution. On the other hand, from the present systematic XAS analyses, we provide clear evidence of a significant effect of local cation substitution upon all the chemical bonds in the superconducting lattice. And it is also revealed that the competing bond model is very effective in explaining such overall changes of chemical bonds induced by the substitution of alliovalent cations. On the basis of these results, we claim that the effect of local substitution on all the present chemical bonds should be carefully investigated for understanding the physical properties of cation-substituted superconducting materials.

ACKNOWLEDGMENT

This work was supported by the Korean Ministry of Education (Grant No. BSRI-97-3413) and in part by the Korean Science and Engineering Foundation through the Center for Molecular Catalysis. The authors are grateful to Professor M. Nomura for helping us to obtain the XAS data in the Photon Factory.

*To whom all correspondence should be addressed. Electronic address: jhchoy@plaza.snu.ac.kr

[1] J.-H. Choy, N.-G. Park, S.-J. Hwang, D.-H. Kim, and N. H. Hur, J. Am. Chem. Soc. **116**, 11 564 (1994); J.-H. Choy, S.-J. Hwang, and N.-G. Park, *ibid.* **119**, 1624 (1997); J.-H. Choy, S.-J. Hwang, and D.-K. Kim, Phys. Rev. B **55**, 5674 (1997).

[2] J. M. Wheatley, T. C. Hsu, and P. W. Anderson, Nature (London) **333**, 121 (1988); X.-D. Xiang, W.-A. Vareka, A. Zettl, J.-L. Corkill, T. W. Barbee III, M.-L. Cohen, N. Kijima, and R. Gronsky, Science **254**, 1487 (1991).

[3] M. K. Bae, M. S. Kim, S. I. Lee, J.-H. Choy, N.-G. Park, S.-J. Hwang, and D.-H. Kim, Phys. Rev. B **53**, 12 416 (1996).

[4] J.-H. Choy, N.-G. Park, S.-J. Hwang, and Z.-G. Khim, J. Phys. Chem. **100**, 3783 (1996).

[5] J.-H. Choy, S.-J. Hwang, D.-H. Kim, and H.-H. Park, Synth. Met. **71**, 1589 (1995).

[6] Y. Koike, Y. Iwabuchi, S. Hosoya, N. Kobayashi, and T. Fukase, Physica C **159**, 105 (1989).

[7] D. B. Mitzi, L. W. Lombardo, A. Kapitulnik, S. S. Laderman, and R. D. Jacowitz, Phys. Rev. B **41**, 6564 (1990).

[8] M. Kikuchi, H. Nameki, Y. Syono, R. Suzuki, M. Nagoshi, S. Awaji, and N. Kobayashi, Physica C **185–189**, 683 (1991).

[9] Y. Idemoto, H. Tokunaga, and K. Fueki, Physica C **231**, 37 (1994).

[10] S. K. Agarwal andA. V. Narlikar, Prog. Cryst. Growth Charact. **28**, 219 (1994).

[11] J. M. Tranquada, A. H. Mouden, A. I. Goldman, P. Zolliker, D. E. Cox, G. Shirane, S. K. Sinha, D. Vaknin, D. C. Johnston, M. S.

Alvarez, and A. J. Jacobson, Phys. Rev. B **38**, 2477 (1988).
[12] J. B. Torrance, Y. Tokura, A. I. Nazzal, A. Bezinge, T. C. Huang, and S. S. P. Parkin, Phys. Rev. Lett. **61**, 1127 (1988).
[13] A. Maeda, M. Hase, I. Tsukada, K. Noda, S. Takebayashi, and K. Uchinokura, Phys. Rev. B **41**, 6418 (1990).
[14] A. Manthiram, X. X. Tang, and J. B. Goodenough, Phys. Rev. B **42**, 138 (1990).
[15] J.-H. Choy, D.-K. Kim, G. Demazeau, and D.-Y. Jung, J. Phys. Chem. **98**, 6258 (1994).
[16] J.-H. Choy, D.-K. Kim, S.-H. Hwang, G. Demazeau, and D. Y. Jung, J. Am. Chem. Soc. **117**, 8557 (1995).
[17] A. Manthiram and J. B. Goodenough, Appl. Phys. Lett. **53**, 2695 (1988).
[18] J. G. Bednorz and K. A. Muller, Z. Phys. B **64**, 189 (1986).
[19] Y. Tokura, H. Takagi, and S. Uchida, Nature (London) **337**, 345 (1989).
[20] H. Oyanagi, T. Matsushida, M. Ito, and H. Kuroda, KEK Report No. 83, 1984 (unpublished), p. 30; H. Kuroda and A. Koyama, KEK Report No. 84, 1989 (unpublished), p. 19.
[21] F. W. Lytle, G. van der Laan, R. B. Greegor, E. M. Larson, C. E. Violet, and J. Wong, Phys. Rev. B **41**, 8955 (1990).
[22] E.-A. Stern and K. Kim, Phys. Rev. B **23**, 3781 (1981).
[23] B. K. Teo, *EXAFS: Basic Principles and Data Analysis* (Springer-Verlag, Berlin, 1986).
[24] J. E. Hahn, R. A. Scott, K. O. Hodgson, S. Doniach, S. R. Desjardins, and E. I. Solomon, Chem. Phys. Lett. **88**, 595 (1982).
[25] J.-H. Choy, D.-K. Kim, S.-H. Hwang, and G. Demazeau, Phys. Rev. B **50**, 16 631 (1994).
[26] R. A. Bair and W. A. Goddard III, Phys. Rev. B **22**, 2767 (1980); N. Kosugi, H. Kondoh, H. Tajima, and H. Kuroda, Chem. Phys. **135**, 149 (1980).
[27] J.-H. Choy, D.-K. Kim, and J.-C. Park, J. Am. Chem. Soc. **117**, 7556 (1995).
[28] Although the raw EXAFS spectra are not represented, their qualities are quite good enough to obtain reliable fitting results, regardless of La content (x).
[29] A. Koizumi, H. Maruyama, H. Yamazaki, H. Maeda, T. Ishii, Y. Miura, and J. Takada, Physica C **190**, 338 (1992).
[30] P. P. Lottici, G. Antonioli, and F. Licci, Physica C **152**, 468 (1988).
[31] D. DiMarzio, H. Wiesmann, D. H. Chen, and S. M. Heald, Phys. Rev. B **42**, 294 (1990).
[32] R. D. Shannon, Acta Crystallogr., Sect. A: Cryst. Phys., Diffr., Theor. Gen. Crystallogr. **32**, 751 (1976).
[33] The oxidation of CuO_2 layers upon intercalation is suggested to be either due to a charge transfer between host and guest and/or due to a change in oxygen content induced by the heat treatment during the intercalation reaction. But according to a previous study on the oxygen-loss effect [Phys. Rev. B **43**, 10 445 (1991)], it is clear that the annealing in a vacuum-sealed tube at the low temperature of 230–240 °C does not induce any significant change in the oxygen content of the host lattice and T_c. Therefore, the observed remarkable change in Cu-O_{Sr} bond is completely attributed to a charge transfer between the guest $HgBr_2$ layer and CuO_2 one along the bonds of Bi-O_{Sr}-Cu.
[34] J. B. Goodenough, Prog. Solid State Chem. **5**, 145 (1971).
[35] R. Bottner, N. Schroeder, E. Dietz, V. Gerhardt, W. Assmers, and J. Kowalewsi, Phys. Rev. B **41**, 8679 (1990).
[36] F. Burgazy, H. Jaeger, C. Politis, P. Lamparter, and S. Steeb, in *Electronic Properties of High-T_c Superconductors and Related Compounds*, edited by H. Kuzmany, M. Mehring, and J. Fink (Springer-Verlag, Berlin, 1990), p. 135; J. B. Goodenough and J. Zhou, Phys. Rev. B **42**, 4276 (1990).
[37] E. Kaldis, D. Fisher, A. W. Hewat, E. A. Hewat, J. Karpinski, and S. Rusiecki, Physica C **159**, 668 (1989).
[38] Y. Shimakawa, Y. Kubo, T. Manaka, T. Satoh, S. Iijima, T. Ichihasi, and H. Igarashi, Physica C **157**, 279 (1989).
[39] F. Faiz, G. Jennings, J.-C. Campuzano, E.-E. Alp, J.-M. Yao, D.-K. Saldin, and J.-J. Yu, Phys. Rev. B **50**, 6370 (1994).
[40] F. Studer, D. Bourgault, C. Martin, R. Retoux, C. Michael, B. Raveau, E. Dartyge, and A. Fontaine, Physica C **159**, 609 (1989).
[41] R. Retoux, F. Studer, C. Michael, B. Raveau, A. Fontaine, and E. Dartyge, Phys. Rev. B **41**, 193 (1990).
[42] R. Åkesson, I. Persson, M. Sandstrom, and U. Wahlgren, Inorg. Chem. **33**, 3715 (1994).
[43] T. Yamamura, T. Watanabe, A. Kikuchi, M. Ushiyama, T. Kobayashi, and H. Hirota, J. Phys. Chem. **99**, 5525 (1995).
[44] A.-F. Wells, *Structural Inorganic Chemistry* (Clarendon, Oxford, 1984), p. 444.